Manuscript

Two analytical approaches quantifying the electron donating capacities of dissolved organic matter to monitor its oxidation during chlorination and ozonation

LINDA ÖNNBY[†, a], NICOLAS WALPEN[†, b], ELISABETH SALHI[a], MICHAEL SANDER[b, *] AND URS VON GUNTEN[a, b, c, *]

[†]L. Önnby and N. Walpen contributed equally to this work.

[a]Swiss Federal Institute of Aquatic Science and Technology (Eawag), 8600 Dübendorf, Switzerland

[b]Institute of Biogeochemistry and Pollutant Dynamics, Swiss Federal Institute of Technology (ETH) Zurich, 8092 Zurich, Switzerland

[c]School of Architecture, Civil & Environmental Engineering (ENAC), Ecole Polytechnique Fédérale de Lausanne (EPFL), 1015 Lausanne, Switzerland

Submitted as manuscript to *Water Research*

*Corresponding authors:

Urs von Gunten

E-mail: vongunten@eawag.ch

Phone: +41 58 765 5270

Michael Sander

E-mail: michael.sander@env.ethz.ch

Phone: +41 44 632 8314

Abstract

Electron-donating activated aromatic moieties, including phenols, in dissolved organic matter (DOM) partially control its reactivity with the chemical oxidants ozone and chlorine. This comparative study introduces two sensitive analytical systems to directly and selectively quantify the electron-donating capacity (EDC) of DOM, which corresponds to the number of electrons transferred from activated aromatic moieties, including phenols, to the added chemical oxidant 2,2'-azino-bis(3-ethylbenzothiazoline-6-sulphonate) radical cation (i.e., $ABTS^{\bullet+}$). The first system separates DOM by size exclusion chromatography (SEC) followed by a post-column reaction with $ABTS^{\bullet+}$ and a spectrophotometric quantification of reduction of $ABTS^{\bullet+}$ by DOM. The second system employs flow-injection analysis (FIA) coupled to electrochemical detection to quantify $ABTS^{\bullet+}$ reduction by DOM. Both systems have very low limits of quantification, allowing determination of EDC values of dilute DOM samples with <1 mg carbon per liter. When applied to ozonated and chlorinated model DOM isolates and real water samples, the two analytical systems showed that EDC values of the treated DOM decrease with increasing specific oxidant doses. The EDC decreases detected by the two systems were in overall good agreement except for one sample containing DOM with a very low EDC. The combination of EDC with UV-absorbance measurements gives further insights into the chemical reaction pathways of DOM with chemical oxidants such as ozone or chlorine. We propose the use of EDC in water treatment facilities as a readily measurable parameter to determine the content of electron-donating aromatic moieties in DOM and thereby its reactivity with added chemical oxidants.

Keywords

Electron donating capacity

Dissolved organic matter

Ozonation

Chlorination

Size exclusion chromatography

Flow-injection analysis

Abbreviations

A_{254}:	Absorbance at 254 nm
ABTS:	2,2'-azino-bis(3-ethylbenzothiazoline-6-sulphonate)
$ABTS^{\bullet+}$:	One-electron oxidation product of ABTS
DOC:	Dissolved organic carbon
DOM:	Dissolved organic matter
EDC:	Electron donating capacity
EDC_0:	Electron donating capacity of unaltered DOM
FIA:	Flow-injection analysis
MEO:	Mediated electrochemical oxidation
SEC:	Size exclusion chromatography
$SUVA_{254}$:	Specific UV absorbance at 254 nm

1. Introduction

Dissolved organic matter (DOM) is a complex mixture of low- and high-molecular weight organic molecules originating from various biological precursor materials (Stenson et al. 2003). Because of the diversity of its source materials and extents of biogeochemical processing, DOM covers a wide range of physicochemical properties. In water treatment, DOM interferes with coagulation, membrane filtration, adsorption, and chemical oxidation processes (Amy 2008, Kennedy and Summers 2015, Köhler et al. 2016, Velten et al. 2011, von Sonntag and von Gunten 2012, Yuan and Zydney 1999). In the latter case, DOM is a significant sink for chemical oxidants such as chlorine and ozone and may thus lower the efficiency for disinfection and micropollutant abatement (Deborde and von Gunten 2008, Lee and von Gunten 2016, von Gunten 2003, von Sonntag and von Gunten 2012). While the oxidant dose may be increased to compensate for oxidant consumption by DOM, this may also increase the formation of undesired disinfection by-products (DBPs) from the reaction of the oxidant with DOM. In the case of chlorine, these by-products are potentially carcinogenic (Hammes et al. 2006, Krasner et al. 2013, Lavonen et al. 2013, Richardson 2003, Richardson 2011, Richardson et al. 2007, Zhang and Minear 2006). Reaction of DOM with ozone produces assimilable organic carbon, which in turn leads to biological growth in the treated water (Collins and Vaughan 1995, Escobar and Randall 2001, Hu et al. 1999, Van der Kooij et al. 1989). High ozone exposures also increase bromate formation in bromide-containing waters (von Gunten 2003). Therefore, the oxidant dose has to be optimized for an effective disinfection and abatement of micropollutants while minimizing the DBP formation. For this purpose, the concentration and the reactivity of the DOM plays a crucial role.

A common approach in water treatment for online determination of DOC concentration is the measurement of the UV-visible light absorption of DOM (Her et al. 2002, Huber et al. 2011, Korshin et al. 1997, Leenheer and Croue 2003) or the specific UV-absorbance at 254 nm ($SUVA_{254}$), which is obtained by normalizing the measured absorbance at 254 nm by the DOC concentration. $SUVA_{254}$ is commonly used as a proxy for DOM aromaticity, the fraction of aromatic to total carbon. The $SUVA_{254}$ values of numerous organic matter isolates were found to correlate with aromaticity determined by ^{13}C-NMR (Traina et al. 1990, Weishaar et al. 2003, Westerhoff et al. 1999). Several studies showed that the concentrations of chlorinated DBPs formed by reaction of chlorine with DOM were positively correlated with $SUVA_{254}$ values and that the chlorination of DOM resulted in a decrease in the UV absorbance (Korshin et al. 1997, Reckhow et al. 1990). However, the correlations between $SUVA_{254}$ and DBP formation vary among differing DOM samples and $SUVA_{254}$ has only limited value as a predictor for the formation of DBPs during chlorination of DOM from varying sources (Fram 1999, Weishaar et al. 2003). These limitations were ascribed to $SUVA_{254}$ values providing only a measure for DOM aromaticity but not for the entire fraction of DBP-producing moieties (trihalomethanes, Weishaar et al. 2003). For ozone consumption kinetics during reactions with DOM (natural waters and isolates) no satisfying correlations could be found with $SUVA_{254}$ (Elovitz et al. 2000). Nevertheless, UV absorbance changes during ozonation have been successfully applied as a surrogate parameter for the abatement of micropollutants during enhanced wastewater ozonation (Bahr et al. 2007, Wert et al. 2009). This approach is based on the competition for ozone consumption between chromophoric DOM reactive sites and micropollutants.

We recently introduced mediated electrochemical oxidation (MEO) to quantify electron-donating activated aromatic moieties (mostly phenols) in DOM (Aeschbacher et al. 2009, Aeschbacher et al. 2011). This method relies on the electrochemical quantification of the number of electrons transferred from DOM to the radical cation of 2,2'-azino-bis(3-ethylbenzothiazoline-6-sulphonate) (i.e., $ABTS^{\bullet+}$). $ABTS^{\bullet+}$ was used as chemical oxidant because it has a sufficiently high standard reduction potential ($E_H^0(ABTS^{\bullet+}/ABTS)$= 0.7 V) (Scott et al. 1993) to oxidize phenols and is readily reduced in a pH-independent, reversible one-electron transfer. The number of electrons transferred from DOM to $ABTS^{\bullet+}$ per mass of DOM is referred to as the electron donating capacity (EDC). While the EDC is operationally defined (i.e., EDC increases with increasing pH, E_H and reaction time, (Aeschbacher et al. 2012)), the EDC values of a diverse set of model DOM isolates were found to linearly correlate with their titrated phenol contents (Aeschbacher et al. 2012). We quantified changes in the EDC of DOM upon oxidation with chlorine dioxide (ClO_2), chlorine (HOCl) and ozone (O_3) (Wenk et al. 2013). We demonstrated that chlorination resulted in pronounced decreases in EDC values but comparatively small decreases in $SUVA_{254}$ values, suggesting that chlorine primarily reacted by electrophilic aromatic substitution leading to chlorophenols, which still absorb UV light, but cannot be oxidized by $ABTS^{\bullet+}$. Ozonation of the same DOM resulted in more comparable relative EDC and absorbance losses, suggesting that ozone reacted by electrophilic addition to aromatic structures, followed by ring cleavage (Ramseier and von Gunten 2009). These findings demonstrated that MEO allows quantifying changes in DOM redox state during chemical oxidation and –in combination with $SUVA_{254}$ measurements– provided insights into possible oxidation pathways of DOM. This is further supported by a recent study in which the decreases in both EDC

and $SUVA_{254}$ during DOM ozonation were applied as proxies for micropollutant abatement and bromate formation (Chon et al. 2015). Furthermore, in a chemical oxidation study of low molecular weight model phenols, EDC was shown to correlate with chlorine demand, suggesting that monitoring EDC during chemical water treatment may help identifying optimal oxidant doses (de Vera et al. 2017).

While these studies demonstrated the usefulness of EDC for monitoring the oxidation state of DOM during chemical oxidation and determining DOM oxidant demand, the original MEO method (Aeschbacher et al. 2010, Aeschbacher et al. 2012) required advancements on two levels for a more widespread application during oxidative water treatment: an automated sample analysis and an improved sensitivity to quantify EDC under realistic conditions. To this end, two analytical methods have recently been introduced. First, an LC-based system in which DOM is first passed through a SEC column followed by post-column oxidation of DOM by preformed $ABTS^{\bullet+}$. The extent of reduction of $ABTS^{\bullet+}$ was quantified based on the loss of absorbance of $ABTS^{\bullet+}$ at 405 nm (Chon et al. 2015). Second, a flow-injection analysis (FIA) system in which DOM is reacted with electrochemically-generated $ABTS^{\bullet+}$, followed by chronoamperometric –instead of a spectrophotometric– detection in an electrochemical flow-through detector to quantify of the extent of $ABTS^{\bullet+}$ reduction by DOM (Walpen et al. 2016). While both methods were shown to reliably determine EDC in water samples with low DOM concentrations, a systematic investigation of the capabilities of the methods to monitor chemical DOM oxidation was missing.

The objective of this study was to provide a systematic assessment of the performances of the two analytical methods, subsequently abbreviated as SEC-EDC and FIA-EDC, to quantify decreases in the EDC of diverse DOM samples upon chemical oxidation. To this end, we treated water samples containing DOM with

different doses of ozone or chlorine and quantified the resulting losses in EDC using the two methods. To span a wide range of DOM characteristics, the treated samples included solutions prepared from three model DOM isolates and three real water samples collected in Switzerland and in Sweden. Based on the results, we evaluate the applicability of the two MEO methods in water treatment facilities to monitor DOM oxidation during chlorination and ozonation.

2. Material and methods

2.1 Chemicals

The chemicals used in the study are listed in the Supplementary Material in Appendix A.

2.2 DOM samples

2.2.1 Model DOM isolates

Three model DOM isolates were obtained from the International Humic Substances Society (St. Paul, Minnesota, USA) and used as received: Pony Lake Fulvic Acid (PLFA, 1R109F), Nordic Lake Aquatic Natural Organic Matter (NNOM, 1R108N) and Suwannee River II Standard Fulvic Acid (SRFA, 2S101F). We selected these three isolates because they cover a range of physicochemical properties and have different origins. Detailed information on the isolates, including selected chemical characteristics (aromaticity and elemental composition), are provided in **Table S1**.

Stock solutions of the DOM isolates were prepared by dissolving the material in unbuffered, ultrapure water (approximately 50 $mg_C \cdot L^{-1}$). The exact concentration of each stock solution was determined by diluting aliquots 10- and 50-fold in phosphate buffer (5 mM phosphate buffer, pH 7; 0.1 M NaCl), measuring the

195 absorption coefficient at 254 nm (a_{254}) using a spectrophotometer (Cary 100, Varian,
196 USA) and calculating the DOC concentration from predetermined $SUVA_{254}$ values
197 (**Table S2**).

198 2.2.2 Real water samples

199 Three real water samples were included in this study to investigate chemical
200 oxidation of DOM that have not been pre-extracted. The first sample was collected
201 from the wastewater effluent (WWE after biological treatment (Bourgin et al. 2018))
202 of the wastewater treatment plant Neugut in Dübendorf, Switzerland. The other two
203 samples were collected from the surfaces of Lake Sjököp (SLW) and Lake Vomb
204 (VLW) in Sweden. We selected Lake Sjököp because it has high DOC
205 concentrations, presumably due to organic matter input from a peatland surrounding
206 the lake. In contrast, Lake Vomb is a drinking water source with low DOC
207 concentrations. The exact sampling locations and selected physicochemical properties
208 of the samples (pH, DOC, and $SUVA_{254}$) are provided in **Table S3**. The water
209 samples were filtered through pre-rinsed cellulose nitrate membranes (0.45-µm pore
210 size; Sigma Aldrich, Switzerland) on the day they were collected to remove
211 particulate organic matter and microorganisms. The samples were stored at 4 °C in
212 the dark until use (within 10 days of sampling). The absorbance spectrum of the
213 filtered real water samples did not change between sampling and analysis, suggesting
214 minimal if any microbial degradation of the DOM during sample storage.

215 **2.3 Chemical oxidation of DOM**

216 We used a commercially available hypochlorite solution (6-14%) to prepare
217 chlorine stock solutions (10 mM HOCl) in unbuffered, ultrapure water. The exact
218 chlorine concentrations of the stocks were determined spectrophotometrically either
219 by absorbance measurements at 290 nm (ε_{290}= 350 $M^{-1} \cdot cm^{-1}$ (Soulard et al. 1981)) or

220 by reaction with *N*,*N*-diethyl-p-phenylenediamine (DPD) followed by quantification
221 of the oxidation product of DPD by absorbance measurement at λ = 515 nm
222 (American Public Health Association, 2012).

223 Ozone stock solutions of approximately 1.5 mM ozone were obtained with an
224 ozone generator (Innovatec CMG 3-3 ozone generator (Rheinbach, Germany)) from
225 pure oxygen. The generated ozone gas was sparged through unbuffered, ultrapure
226 water cooled on ice. The exact ozone concentration in the resulting stock solutions
227 was determined spectrophotometrically at 260 nm (ε_{260}= 3200 $M^{-1} \cdot cm^{-1}$ (von Sonntag
228 and von Gunten 2012)) or by reaction with indigo (Bader and Hoigné 1981, von
229 Sonntag and von Gunten 2012).

230 Prior to the chemical oxidation with chlorine or ozone, the model DOM isolate
231 stock solutions were diluted to 2.5 $mg_C \cdot L^{-1}$ in phosphate buffer (final phosphate
232 concentration: 10 mM; pH 7). The real water samples were diluted to 2.5 $mg_C \cdot L^{-1}$
233 with ultrapure water and subsequently adjusted to pH 7 using HCl (0.2 M; a final
234 concentration of 24 and 45 µM of HCl was required for VLW and WWE,
235 respectively). We oxidized the DOM solutions by adding a defined volume of the
236 oxidant stock solutions to obtain the desired specific oxidant dose from 0 to 0.2
237 $mol_{HOCl} \cdot mol_C^{-1}$ for chlorine and from 0 to 0.5 $mol_{ozone} \cdot mol_C^{-1}$ for ozone. We stored the
238 ozonated samples at room temperature for 24 h and stored the chlorinated samples in
239 the dark for 48 h at room temperature, to ensure complete reaction of the respective
240 oxidant prior to sample analyses. Complete reaction was confirmed by control
241 measurements of the residuals of the respective oxidant. All experiments were carried
242 out in the presence of *t*-BuOH (100 mM). In ozonation experiments, *t*-BuOH served
243 to quench hydroxyl radicals, which are formed during ozone decay (von Sonntag and

von Gunten 2012). To match the solution matrix of the ozonation experiments, chlorination experiments were also run in the presence of 100 mM *t*-BuOH.

2.4 Quantification of EDC of DOM samples

Figure 1 shows a scheme of the two analytical system setups to quantify EDC, SEC-EDC and FIA-EDC. The components and the sample analysis principles of the two systems are described in the following.

2.4.1. SEC-EDC system

The SEC-EDC system was briefly described in a previous publication (Chon et al. 2015). In this system, DOM samples (volume: 2.5 mL) were analyzed using a high performance liquid chromatography system (Ultimate 3000, Thermo Fisher Scientific) connected to a SEC column (8 mm x 300 mm, Toyopearl HW50S, Tosoh Bioscience, Japan) packed with macroporous hydroxylated methacrylic polymer beads with a mean bead diameter of 35 µm. The eluent consisted of 50 mM borate at pH 7.8 with a flow rate of 0.2 $mL \cdot min^{-1}$. The SEC column had an exclusion limit of 80'000 Da (Tosoh Bioscience, 2018). Following SEC, the solution passed through a UV detector (PDA 3000, Thermo Fisher Scientific). The SEC column was used to separate DOM from dissolved ions in the injected solution that may affect the reaction of DOM with $ABTS^{\bullet+}$ in the post-SEC reaction. The solution was then passed through a mixing tee, in which the $ABTS^{\bullet+}$ reactant solution was mixed in at a flow rate of 50 $\mu L \cdot min^{-1}$. The $ABTS^{\bullet+}$ reactant solution was delivered pneumatically (PC10, Dionex, USA) from a reservoir to the mixing tee and was prepared by adding sodium hypochlorite sub-stoichiometrically to ABTS (Chon et al. 2015, Pinkernell 2000). The combined SEC-effluent and the reactant solution had a pH of 7.8 and were passed through a knitted polytetrafluoroethylene (PTFE) reaction coil (Dionex, USA; internal volume of 750 µL, corresponding to a delay time of 3 min), in which $ABTS^{\bullet+}$ was

reduced by electron transfer from electron-donating moieties of the DOM. The extent of $ABTS^{\bullet+}$ reduction was subsequently quantified spectrophotometrically in a flow-through cell (path length: 1 cm, UltiMate 3100 VWD UV-detector, Thermo Fisher Scientific) in which the absorbance at 405 nm was continuously recorded. $ABTS^{\bullet+}$ has a strong absorbance at 405 nm, whereas the reduced species, ABTS, shows negligible absorbance at this wavelength (Pinkernell et al. 1997).

The EDC was calculated from the absorbance loss peaks at 405 nm as follows (eq. 1):

$$\mathrm{EDC} = -\frac{1}{m_C} \cdot \left(q_V \cdot \frac{\int \left(A_{405}(t) - A_{405,baseline}\right) \mathrm{d}t}{\varepsilon_{405} \cdot l} \right) \qquad \text{Eq. 1}$$

where m_C is the mass of carbon injected, q_V is total volumetric flow rate passing through the detector ($2.5 \cdot 10^{-3}$ $L \cdot min^{-1}$), ε_{405} is the molar absorption coefficient of $ABTS^{\bullet+}$ at 405 nm (ε_{405} = 31'600 $M^{-1} \cdot cm^{-1}$) (Pinkernell et al. 1997), l is the optical path length of the flow cell (1 cm), A_{405} is the absorbance measured at 405 nm, and $A_{405,\,baseline}$ is the baseline absorbance measured at 405 nm (i.e., the absorbance in the absence of a sample). The term in parenthesis on the right side of equation 1 converts the $ABTS^{\bullet+}$ absorbance loss peak to moles of electrons donated by the injected DOM sample to $ABTS^{\bullet+}$. This conversion from a concentration dependent reading (i.e., absorbance) to an absolute amount of substance converted (i.e., $ABTS^{\bullet+}$ reduced) is well established for spectrophotometric detections on flow injection analysis systems and is considered to also apply to the SEC-EDC system studied herein.

(Figure 1)

2.4.2 FIA-EDC system

We used a previously described FIA system (Walpen et al. 2016) to quantify EDC values of DOM samples (**Figure 1**). Briefly, DOM samples were sequentially

loaded through a 11-port/10-position selector valve into a sample loop (volume 100 µL) of a 10-port/2-position injector valve, from which they were injected into a buffered carrier stream (pH 7, 100 mM phosphate; $q_{carrier}$ = 75 µL·min^{-1}). The carrier stream was delivered to a mixing tee where it was continuously mixed with the reagent stream ($q_{reagent}$ = 15 µL·min^{-1}). The reagent stream contained electrochemically produced ABTS$^{\bullet+}$ (450 µM) and was weakly buffered to pH 4 (1 mM acetate, 100 mM KCl) at which ABTS$^{\bullet+}$ was stable (note that the stability of ABTS$^{\bullet+}$ decreases with increasing pH (Walpen et al. 2016)). The combined carrier and reagent solutions were then delivered through a knitted PTFE reaction coil (Biotech, Sweden) with an internal volume of 2 mL, corresponding to a reaction time of 22 min. The extent of reduction of ABTS$^{\bullet+}$ by DOM was quantified amperometrically in an electrochemical flow cell with a glassy carbon working electrode (ALS, Japan). The working electrode in the detector was polarized to the E_H measured in the solution in the absence of injected samples (i.e., the open-circuit potential defined by the ABTS$^{\bullet+}$/ABTS couple in solution; E_H= +0.71 ± 0.01 V), resulting in background currents <10 nA. Electron transfer from DOM to ABTS$^{\bullet+}$ lowered the ratio of ABTS$^{\bullet+}$ to ABTS and hence the E_H of the solution relative to the E_H applied to the working electrode. The E_H offset led to the oxidation of ABTS and hence oxidative current peaks.

To calibrate the current response of the electrochemical detector, we injected solutions containing the redox standard ascorbate ($EDC_{ascorbate}$= 2.00 $mol_{e-}\cdot mol_{ascorbate}^{-1}$ (Walpen et al. 2018)) at concentrations of 10, 5, 1 and 0 µM. The calibration curve of oxidative current peak area versus number of electrons donated by ascorbate to ABTS$^{\bullet+}$ was used to convert the measured oxidative current responses of DOM samples to EDC values according to the following equation:

$$\mathrm{EDC} = -\frac{1}{m_C} \cdot \frac{\mathrm{EDC}_{ascorbate}}{a_{ascorbate}} \cdot \int (I(t) - I_{baseline})\mathrm{d}t \qquad \text{Eq. 2}$$

where m_C is the mass of carbon injected, $a_{ascorbate}$ ($C \cdot mol_{ascorbate}^{-1}$) is the slope of the linear calibration curve of the area of the oxidative current peaks from the injections of ascorbate standards (see above), I is the oxidative current in response to an injected sample, and $I_{baseline}$ is the oxidative current baseline (i.e., the oxidative current in the absence of an injected sample).

The $ABTS^{\bullet+}$ reagent solution was prepared by direct electrochemical oxidation of an ABTS solution (total ABTS concentration of 750 µM, pH 4 (1 mM acetate)) in an electrochemical cell with a glassy carbon cylinder as working electrode polarized to a reduction potential of E_H= 0.82 V until the concentration of $ABTS^{\bullet+}$ reached 450 µM (Walpen et al. 2016).

All electrochemical analyses were controlled with an electrochemical analyzer (630D, CH Instruments, Austin, TX, USA). All reduction potentials (E_H) were measured against Ag/AgCl reference electrodes but are reported relative to the standard hydrogen electrode.

We conducted the FIA measurements and prepared the reagent and redox standard stock solutions inside an anoxic glove box (N_2 atmosphere, O_2 < 2.3 ppm) with anoxic water. Water and buffer solutions were sparged with N_2 for two hours before transferring them into the glove box. The DOM samples were sparged for 15 min with N_2 prior to being transferred into the glove box. The DOM samples were diluted outside the glovebox two- to four-fold in concentrated phosphate buffer (200 mM) in order to match the carrier buffer (100 mM phosphate).

3. Results and discussion

3.1 Performance assessment of the SEC-EDC system

3.1.1. Size separation of DOM on the SEC column

We assessed size separation of the three model DOM isolates (i.e., SRFA, NNOM and PLFA) on the SEC column in the SEC-EDC system by continuously monitoring the absorbance of the SEC column eluates at 254 nm. **Figure 2** shows representative area-normalized absorbance traces that resulted from the injections of the three DOM isolates (injection volumes of 2.5 mL of solutions with DOM concentrations of 2 $mg_C \cdot L^{-1}$). All three DOM isolates eluted between 30 or 35 and 65 min after injection in the form of broad peaks. SRFA and NNOM started to elute from the SEC column approximately 30 min, whereas PLFA eluted at approximately 35 min after injection. This finding suggests that the largest molecules in PLFA were smaller than those in SRFA and NNOM. The broad chromatographic peaks of all three DOM isolates are consistent with the wide molecular size distributions of DOM (Chin et al. 1994, Huber et al. 2011) and demonstrated their separation on the SEC. A detailed discussion of the separation is provided in the Supplementary Material in which we compare the SEC-EDC system to a previously published SEC system (Huber et al. 2011).

(Figure 2)

3.1.2. Linearity in the response on SEC-EDC system

The SEC-EDC system quantifies the oxidation states of injected DOM by determining the extent to which electron-donating moieties in the DOM reduce $ABTS^{\bullet+}$ to ABTS, which results in a solution absorbance loss at 405 nm. We established linearity in the absorbance loss at 405 nm with increasing injected

concentrations of the model DOM isolates. **Figure 3a** shows the baseline-corrected absorbance loss peaks, which increased in size as the injected amount of SRFA increased from 1.25 to 7.5 μg_C (i.e., 2.5 mL of SRFA solution standards with concentrations from 0.5 to 3.0 $mg_C \cdot L^{-1}$). Similarly, injections of increasing amounts of NNOM and PLFA resulted in increasing sizes of the absorbance loss peaks (**Figure S2** and **S3** (SM) for PLFA and NNOM, respectively). For all three DOM isolates, the areas of the absorbance loss peaks increased linearly with increasing injected amounts of DOM (**Figures 3b** for SRFA and **S2** and **S3** for PLFA and NNOM, respectively; the R^2-values of linear regression fits were 0.994, 0.985 and 0.992 for SRFA, PLFA and NNOM, respectively).

We converted the areas of the absorbance loss peaks to number of electrons transferred to $ABTS^{\bullet+}$ and, subsequently, to the EDC of SRFA, NNOM, and PLFA (**Equation 1)**. The obtained EDC values were positively correlated to the EDC for the same DOM isolates reported determined by MEO (Aeschbacher et al. 2012). At the same time, the EDC values quantified by SEC-EDC were approximately 43% of the values determined by MEO (**Figure S4**). These smaller values reflected the relatively short reaction time of 3 min between DOM and $ABTS^{\bullet+}$ in the reaction coil of the SEC-EDC system. It has previously been demonstrated that EDC values increase with increasing reaction times between DOM and $ABTS^{\bullet+}$ in a reaction coil and that reaction times >20 min are needed to approach EDC values obtained by MEO (Walpen et al. 2016). While the reaction time on the SEC-EDC system can be increased by increasing the length of the reaction coil (or by decreasing the volumetric flow rate), such measures would increase the time for analysis per sample. Also, we subsequently report and discuss decreases in the EDC of DOM during chemical oxidation in relative instead of in absolute terms by normalizing EDC of

389 treated samples to the EDC of the respective untreated DOM sample (see sections 3.3
390 and 3.4). This normalization allows comparing the two analytical methods with
391 regards to the trends in the EDC values of treated samples.

392 The absorbance loss peaks in **Figure 3a** and **Figures S2a** and **S3a** indicate
393 that the limit of quantification (LOQ) for EDC on the SEC-EDC system was below
394 1.25 μg_C. At an injection volume of 2.5 mL, this amount corresponds to solutions
395 with a concentration of 0.5 $mg_C \cdot L^{-1}$. We therefore expected that the sensitivity of the
396 SEC-EDC system was sufficiently high to allow quantifying changes in DOM redox
397 states during chemical oxidation in real water samples, as demonstrated in section 3.4.

398 **(Figure 3)**

399 **3.2 Performance assessment of the FIA-EDC system**

400 In the FIA-EDC system, the DOM sample is directly injected into a carrier
401 stream, which is continuously mixed with a reagent solution containing $ABTS^{\bullet+}$.
402 Reduction of $ABTS^{\bullet+}$ to ABTS by DOM in the reaction coil lowers the
403 $E_H(ABTS^{\bullet+}/ABTS)$ in solution relative to the E_H applied to the working electrode of
404 the electrochemical flow-through detector, thereby giving rise to an oxidative current
405 response. **Figure 3c** shows oxidative current peaks that resulted from successive
406 injections of increasing amounts of SRFA into the FIA-EDC system. Both the peak
407 heights (not shown) and areas (**Figure 3d**) increased linearly with increasing injected
408 amounts of SRFA.

409 To quantify the absolute EDC value of SRFA from this data, we calibrated the
410 FIA system using the oxidative current responses obtained from injecting different
411 amounts of the redox standard ascorbate with EDC= 2.00 $mol_{e^-} \cdot mol_{ascorbate}^{-1}$ (current
412 responses also shown in **Figure 3c**). This calibration was necessary because the

working electrode in the electrochemical flow cell only senses the solution in close proximity to its surface. Using equation 2, we converted the linear regression line in **Figure 3d** to an EDC of SRFA of 5.75 ± 0.19 $mmol_{e^-} \cdot g_C^{-1}$. This value and the EDC values of PLFA (2.15 ± 0.06 $mol_{e^-} \cdot g_C^{-1}$) and NNOM (4.15 ± 0.13 $mol_{e^-} \cdot g_C^{-1}$) quantified on the FIA-EDC system were in very good agreement with the EDC of the same DOM isolates previously quantified by MEO at pH 7 and an applied reduction potential of E_H= 0.71 V (Aeschbacher et al. 2012) (see **Figure S4**). The good agreement of EDC quantified by FIA-EDC and MEO show that the 22 min reaction time of the model DOM isolates with $ABTS^{\bullet+}$ in the reaction coil of the FIA-EDC system was sufficiently long to approach the EDC determined in MEO with an approximate reaction time of 40 min (Aeschbacher et al. 2012).

We previously determined a limit of quantification (LOQ) on the FIA-EDC system of approximately 10 to 50 ng_C for model DOM isolates (depending on their EDC) (Walpen et al. 2016). This LOQ range is in good agreement with the oxidative current peak in **Figure 3c** in response to the smallest injected amount of SRFA of 190 ng_C (well above the LOQ). With an injection volume of 100 µL, the LOQ of 10 to 50 ng_C corresponds to solutions with DOM concentrations of 0.1 to 0.5 $mg_C \cdot L^{-1}$. This range is at the lower end of DOM concentrations for many natural water samples, suggesting that the FIA-EDC system allows quantifying changes in DOM redox states during chemical oxidation of natural DOM water samples, as demonstrated in section 3.4.

3.3 Effects of ozonation and chlorination on redox states of model DOM isolates

Figure S5 shows the changes in the absolute EDC values of the model DOM isolates upon treatment with ozone and chlorine, as quantified by FIA-EDC. In the following discussion, we report the EDC of DOM treated at a specific oxidant dose

438 relative to the EDC of the respective untreated DOM (EDC_0) (i.e., $EDC \cdot (EDC_0)^{-1}$).
439 This normalization allows comparing results from the SEC-EDC and FIA-EDC
440 systems, despite the different absolute EDC that these systems quantify for the same
441 DOM sample (**Figure S4**).

442 3.3.1 Effect of ozonation on EDC of model DOM isolates

443 We exposed all three model DOM isolates to increasing specific ozone doses
444 (from 0.05 to 0.5 $mol_{ozone} \cdot mol_C^{-1}$), followed by quantifying the resulting changes in
445 EDC of the treated DOM samples. On both the SEC-EDC and FIA-EDC systems, the
446 $EDC \cdot (EDC_0)^{-1}$ of the treated DOM decreased with increasing specific ozone doses
447 (**Figure 4a, b**). At the highest specific ozone dose of 0.5 $mol_{ozone} \cdot mol_C^{-1}$, the EDC
448 values had decreased to between 20 and 5% of the EDC of the untreated DOM
449 samples. The pronounced decreases in $EDC \cdot (EDC_0)^{-1}$ demonstrate that reaction of the
450 added ozone with the DOM resulted in the loss of electron-donating moieties, most
451 likely activated aromatic moieties, including phenols. These results are consistent
452 with previous studies which reported that ozonation of DOM samples decreased their
453 EDC (Chon et al. 2013, Wenk et al. 2013).

454 The decrease in $EDC \cdot (EDC_0)^{-1}$ with increasing specific ozone doses was
455 approximately linear at the lower doses but leveled off at non-zero values for higher
456 ozone doses (**Figure 4a, b**). Per unit of ozone added, more electron-donating moieties
457 in the DOM were therefore lost at the lower than at the higher specific ozone doses.
458 This dose dependency in the EDC indicated that a small fraction of the electron-
459 donating moieties was resistant to reaction with ozone and thus remained in the DOM
460 even at the highest tested ozone doses.

461 **(Figure 4)**
462

463 3.3.2 Effect of chlorination on EDC of model DOM isolates

464 Consistent with the results of ozonation, analysis of chlorinated model DOM
465 isolates on both the SEC-EDC and the FIA-EDC systems showed decreasing
466 $EDC \cdot (EDC_0)^{-1}$ for the three DOM isolates with increasing specific HOCl doses
467 (**Figure 4c, d**). This finding is consistent with earlier work which used MEO and
468 more concentrated DOM solutions to show that chlorination of three model DOM
469 isolates decreased their EDC (Wenk et al. 2013). At the highest chlorine dose of 0.2
470 $mol_{HOCl} \cdot (mol_C)^{-1}$, only the responses to injections of SRFA, the model DOM with the
471 highest initial EDC, were sufficiently large on both the SEC-EDC and FIA-EDC
472 systems to allow for an accurate quantification of residual EDC.

473 On both analysis systems, the $EDC \cdot (EDC_0)^{-1}$ of all three model DOM isolates
474 appeared to decrease in a more linear fashion with increasing specific HOCl dose as
475 compared to the decreases in $EDC \cdot (EDC_0)^{-1}$ during ozonation. The more linear
476 decrease in $EDC \cdot (EDC_0)^{-1}$ during chlorination may have reflected increasing extents
477 of chlorination of phenolic moieties in the DOM with increasing specific HOCl doses
478 (Gallard and von Gunten 2002, Wenk et al. 2013). Such (poly)chlorinated phenolic
479 moieties form by electrophilic attack of HOCl on the phenolic moiety of the DOM.
480 The attack initially starts at the *ortho*- and *para*-position of the phenols, and continues
481 with a gradual increased chlorination of the phenol moieties in the DOM. It can be
482 expected that formed (poly)-chloro-phenols are less oxidizable by $ABTS^{\bullet+}$ and thus
483 led to decreasing $EDC \cdot (EDC_0)^{-1}$.

3.4 Effects of ozonation and chlorination on redox states of real water DOM samples

3.4.1 Quantification of EDC of DOM in real water samples

We first quantified the absolute EDC values of the DOM in the three real water samples (at concentrations of 2.5, 2.5 and 3.85 $mg_C \cdot L^{-1}$ for SLW, VLW and WWE, respectively) using the FIA-EDC system. The specific EDC values decreased in the order SLW (4.86 $mmol_{e^-} \cdot (g_C)^{-1}$) > WWE (3.72 $mmol_{e^-} \cdot (g_C)^{-1}$) > VLW (1.17 $mmol_{e^-} \cdot (g_C)^{-1}$). The high EDC value of SLW likely reflects that the lake from which the sample was collected contained (poly)phenolic DOM from the nearby peatland. We previously showed that DOM from peatlands has exceptionally high EDC as compared to aquatic and terrestrial model DOM isolates (Walpen et al. 2018, Walpen et al. 2016). By contrast, VLW had a lower EDC than any other DOM we previously analyzed ((Aeschbacher et al. 2012)Walpen et al. 2018, Walpen et al. 2016). This finding suggests that the DOM of VLW had a very low concentration of oxidizable, activated aromatic moieties consistent also with its very low $SUVA_{254}$ value (**Table S3**) as compared to previously analyzed aquatic model DOM isolates (Walpen et al. 2016). While the $SUVA_{254}$ of WWE was even smaller than that of VLW, it had a much higher EDC, indicating that this DOM had a comparatively high content of hydroxylated aromatic rings.

3.4.2 Effect of ozonation on EDC in real water samples

Ozonation of real water samples showed decreasing $EDC \cdot (EDC_0)^{-1}$ on both the SEC-EDC and the FIA-EDC systems for increasing specific ozone doses (**Figure 5a, b**). This finding implies that (i) ozonation resulted in a loss of electron-donating moieties also in DOM in real water samples (and not only from model DOM isolates

dissolved in the laboratory, as shown in sections 3.3.1 and 3.3.2) and (ii) both systems can be used to measure these losses. Similar to the observation for model DOM isolates, the $EDC \cdot (EDC_0)^{-1}$ decreased linearly with increasing specific ozone doses at low doses but leveled off at higher doses.

On the SEC-EDC system, the $EDC \cdot (EDC_0)^{-1}$ of WWE and VLW decreased to <20% for the sample with the highest specific ozone dose. The abatement of these moieties appeared less efficient in SLW, for which $EDC \cdot (EDC_0)^{-1}$ decreased to only about 40% for the highest ozone dose. Analyses of the same samples on the FIA-EDC system showed comparable relative EDC decreases with increasing specific ozone doses for SLW and WWE. However, the measured decreases in EDC for VLW upon ozonation were much smaller on the FIA-EDC system. We will discuss potential causes for this apparent discrepancy between the two analytical systems in section 3.5.

(Figure 5)

3.4.3 Effect of chlorination on EDC in real water samples

Similar to the effects of ozonation, SEC-EDC and FIA-EDC analyses of the chlorinated real water samples showed decreasing $EDC \cdot (EDC_0)^{-1}$ with increasing specific HOCl doses (**Figure 5c, d**), demonstrating that (i) HOCl removed electron donating moieties in the DOM of all three real water samples and (ii) that both analytical systems were capable of monitoring HOCl-induced oxidation of DOM in real water samples. With the exception of VLW on the FIA-EDC system, the decreases in $EDC \cdot (EDC_0)^{-1}$ as a function of the specific HOCl doses again appeared to be more linear than the decreases in $EDC \cdot (EDC_0)^{-1}$ with increasing specific ozone doses. Over the entire range of specific HOCl doses, both analytical systems showed

that chlorination resulted in higher EDC decreases for VLW and WWE than for SLW, suggesting that the latter contained a higher fraction of the total electron donating moieties that did not readily react with HOCl.

The two analytical systems showed a large difference in the decreases in $EDC \cdot (EDC_0)^{-1}$ for VLW (**Figure 5c**, **d**). On the SEC-EDC system, the EDC of VLW decreased continuously with increasing specific HOCl dose to approximately 15% of its initial value at the highest tested chlorine dose of 0.2 $mol_{HOCl} \cdot (mol_C)^{-1}$. Conversely, the EDC values of the same samples measured on the FIA-EDC system decreased more readily with increasing HOCl doses to negative values (i.e., the electrochemical cell yielded reductive instead of oxidative current responses) above a specific HOCl dose of 0.04 $mol_{HOCl} \cdot (mol_C)^{-1}$. Furthermore, the errors in replicate analyses were larger, as shown by the relatively large error bars on the VLW data. These apparent differences in the results generated by the two analytical systems will be discussed in section 3.5.

3.5 Comparison of results from SEC-EDC and FIA-EDC systems

3.5.1 Analyses of ozonated and chlorinated model DOM isolates

To compare the results obtained from the two analytical systems, we plotted the decreases in $EDC \cdot (EDC_0)^{-1}$ of the three model DOM isolates during ozonation and chlorination determined by FIA-EDC (*y*-axis) versus the $EDC \cdot (EDC_0)^{-1}$ decreases of the same samples determined by SEC-EDC (*x*-axis). **Figure 6a** shows that the results from the two analysis systems were in very good agreement for ozonated model DOM isolates (i.e., the data scattered around the 1:1 line). This finding implies that ozonation of the model DOM isolates resulted in similar relative decreases in the contents of DOM moieties that readily donate electrons to $ABTS^{\bullet+}$ during the 3 min in

556 the reaction coil of the SEC-EDC system and of the moieties that reacted with
557 $ABTS^{\bullet+}$ over 25 min in the reaction coil of the FIA-EDC system.

558 While the results from the two systems were also in good overall agreement
559 for chlorinated model DOM isolates (**Figure 6b**), the data of SRFA and PLFA
560 showed more systematic deviations from the 1:1 line. In the case of SRFA, the
561 slightly smaller decreases in $EDC \cdot (EDC_0)^{-1}$ on the FIA-EDC than the SEC-EDC
562 system may have resulted from the longer reaction time of the DOM with $ABTS^{\bullet+}$ in
563 the FIA-EDC system. Chlorination of SRFA likely formed chlorinated phenolic
564 moieties, which had slower reactivities with $ABTS^{\bullet+}$ than the corresponding non-
565 chlorinated moieties. Monochlorinated phenols, which are formed for small chlorine
566 doses, may have been oxidized by $ABTS^{\bullet+}$ in the FIA-EDC system with longer
567 reaction times but not in the SEC-EDC system with shorter reaction times, which
568 explain the observed larger decreases in $EDC \cdot (EDC_0)^{-1}$ on the SEC-EDC than the
569 FIA-EDC system. With higher chlorine doses, where (poly)-chlorinated phenols may
570 be formed, there is no reaction with $ABTS^{\bullet+}$ anymore, and both systems measured
571 low $EDC \cdot (EDC_0)^{-1}$. By increasing the length of the reaction coil and therefore the
572 reaction time of $ABTS^{\bullet+}$ with DOM in the SEC-EDC system this potential cause for
573 the deviation could possibly be eliminated.

574 The slightly smaller decreases in $EDC \cdot (EDC_0)^{-1}$ of chlorinated PLFA on the
575 SEC-EDC than the FIA-EDC system (**Figure 6b**) may indicate that PLFA contains a
576 larger fraction of electron donating moieties that are only slowly oxidized by $ABTS^{\bullet+}$.
577
578

(Figure 6)

3.5.2 Analyses of ozonated and chlorinated real water samples

Similar to the model DOM isolates, analysis of the ozonated and chlorinated SLW and WWE samples on the SEC-EDC and the FIA-EDC systems showed very similar changes in $EDC \cdot (EDC_0)^{-1}$ (**Figure 6c, d**). The agreement between results from the two systems was again very good for the ozonated samples (**Figure 6c**). Slight deviations of data points from the 1:1 line for the chlorinated SLW and WWE (**Figure 6d**) likely resulted from shorter $ABTS^{\bullet+}$ reaction times in the SEC-EDC than the FIA-EDC system, as rationalized above for SRFA (**Figure 6b**).

An overall good agreement could be observed for three model DOM isolates and two real water samples. Only the analysis of ozonated and chlorinated DOM in VLW showed larger differences between the two systems. The decreases in $EDC \cdot (EDC_0)^{-1}$ of VLW with increasing oxidant dose were smaller on the FIA-EDC than on the SEC-EDC system for ozonated samples (**Figure 6c**) but larger for the chlorinated samples (**Figure 6d**). While the cause for this apparent discrepancy between the systems (as well as the very different responses on the systems) remains unidentified, a number of factors likely contributed. First, the DOM in VLW had an exceptionally low EDC, resulting in comparatively small spectrophotometric and amperometric responses close to the LOQ on the SEC-EDC and FIA-EDC systems, respectively. These small responses further decreased with increasing chemical oxidation. Second, it is conceivable that inorganic ions in VLW samples interfered with the electrochemical detection on the FIA-EDC system but not with the spectrophotometric detection on the SEC-EDC system. Finally, it remains a possibility that the differences in the reaction times in the reaction coils of the SEC-

603 EDC and the FIA-EDC system contributed to the apparent discrepancy in the results
604 obtained by the two systems.

605 **3.6 Implications for water treatment and process research**

606 3.6.1 Monitoring chemical oxidation of DOM in water treatment facilities

607 The SEC-EDC and the FIA-EDC systems are capable of detecting changes in
608 the concentrations of electron-donating moieties in DOM, both in samples prepared
609 from model DOM isolates as well as in real water samples, during its chemical
610 oxidation by ozone and chlorine. The sensitivity of analyses on both systems is
611 sufficiently high to be applicable to samples in water treatment facilities with very
612 low DOC concentrations (0.5 - 1 $mg_C \cdot L^{-1}$). Furthermore, both systems allow for
613 automated sample analyses. The presented analytical systems therefore overcome the
614 two major analytical challenges of mediated electrochemical oxidation, the approach
615 previously used to monitor chemical DOM oxidation (Wenk et al. 2013: insufficient
616 sensitivity for low DOM samples and manual sample injection. With the previously
617 applied method, quantification of EDC by MEO required approximately four-fold
618 higher DOM concentrations (i.e., 10 $mg_C \cdot L^{-1}$) and, at the same time, sample volumes
619 of 5 to 7 mL, corresponding to 50 to 70 μg_C per analysis. Both the SEC-EDC and the
620 FIA-EDC systems require much smaller amounts of DOM (i.e., < 1 μg_C; see sections
621 3.1 and 3.2), which highlights their superior sensitivity over MEO and thus their
622 applicability to real water samples with low DOC concentrations. In addition to their
623 higher sensitivity, the SEC-EDC and FIA-EDC systems provide automated sample
624 injection, whereas MEO requires manual sample addition to electrochemical cells.
625 Taken together, both SEC-EDC and FIA-EDC have potential to become central
626 analytical tools to determine changes in the concentrations and reactivity of electron-
627 donating moieties in DOM during chemical water treatment.

For routine EDC analysis in water treatment, we recommend using spectrophotometric rather than electrochemical detection to quantify $ABTS^{\bullet+}$ reduction by DOM. While spectrophotometric measurements are less sensitive, they are insensitive to variations in the conductivity of injected sample solutions and thus more robust than amperometric measurements. The use of an SEC column allows separating DOM from inorganic sample matrix constituents that may interfere with the analysis of the redox state of the DOM (e.g., VLW water). However, the use of an SEC column increases the analysis time (90 min) and thus decreases overall sample throughput. The frequency of sample injection and thus overall sample throughput on a FIA system is limited by sample peak broadening, which increases with the reaction time in the system. The FIA-EDC system used herein had a ten-minute injection interval and a total sample analysis time of 25 min. This is typically sufficient for oxidation processes in water treatment, because the dynamics of changes of raw water quality are in the order of hours to days. For applications that require more frequent sample injections, we recommend segmented-flow analysis coupled to spectrophotometric detection. Such systems would allow for a close-to-real time assessment of the chemical oxidant demand of specific water samples and of changes in the oxidation states of DOM during chemical oxidation.

3.6.2 Mechanistic insights into chemical oxidation of DOM

Changes in DOM oxidation state during ozonation and chlorination are currently inferred from decreases in the DOM absorbance, typically at 254 nm. While these absorbance measurements are a semi-quantitative measure of changes in the contents of aromatic moieties in the DOM, they do not provide (i) information on the contents of activated aromatic moieties that readily react with the chemical oxidants and (ii) further insights into the reaction pathways by which the oxidants react with

653 the activated aromatic moieties. This information is available when complementing
654 absorbance measurements with EDC measurements. We plotted the decreases in the
655 $EDC \cdot (EDC_0)^{-1}$ of the three model DOM isolates with increasing chemical oxidant
656 doses versus the concurrent decreases in the absorbance at 254 nm, A_{254}, normalized
657 to the absorbance of the untreated sample, $A_{254,\,0}$ (**Figure 7**). Ozonation of the DOM
658 isolates resulted in large decreases in both $EDC \cdot (EDC_0)^{-1}$ and $A_{254} \cdot (A_{254,\,0})^{-1}$,
659 consistent with the electrophilic addition of ozone to activated aromatic moieties
660 under ring opening. Conversely, chlorination resulted in comparable decreases in
661 $EDC \cdot (EDC_0)^{-1}$, while the decreases in $A_{254} \cdot (A_{254,\,0})^{-1}$ were much smaller than
662 determined for ozonation. This finding suggests that electron-donating activated
663 aromatic moieties were oxidized under comparatively small losses of aromatic units
664 in the model DOM. Similar distinct effects of ozonation and chlorination on DOM
665 were also previously reported when using MEO to quantify EDC values (Wenk et al.,
666 2014). **Figure 7** also shows that each of the two chemical treatments resulted in
667 comparable trends of $EDC \cdot (EDC_0)^{-1}$ versus $A_{254} \cdot (A_{254,\,0})^{-1}$ decreases for the three
668 different DOM isolates, suggesting that the observed distinct reactivity patterns of
669 ozone and chlorine apply to DOM from different sources and with different
670 physicochemical properties. A more detailed, mechanistic discussion of changes in
671 EDC and A_{254} of the DOM upon ozonation and chlorination is part of a forthcoming
672 publication (Önnby et al. 2018).

673 **(Figure 7)**

674 ## 4. Conclusions

675 This study presents two analytical approaches, SEC-EDC and FIA-EDC, to
676 quantify changes in the EDC of DOM isolates and DOM in real water samples during

677 ozonation and chlorination over a range of specific oxidant doses. The major
678 conclusions are:

679 • The high sensitivity of SEC-EDC and FIA-EDC and linearity in the analytical
680 response allows quantifying changes in the EDC values of DOM in aqueous
681 solutions at concentrations as low as 1 $mg_C \cdot L^{-1}$. The two analytical systems
682 can thus be used to quantify the EDC of DOM in most water samples from
683 natural and engineered systems that typically contain larger DOM contents.
684 • For five out of the six DOM samples studied, analysis of the treated DOM
685 samples on the two systems yielded comparable decreases in the relative EDC
686 with increasing specific oxidant doses. The reduction of $ABTS^{\bullet+}$ by DOM can
687 thus be quantified either spectrophotometrically or electrochemically. For one
688 real water sample with an exceptionally low absolute EDC, the results of the
689 two analytical systems deviated from each other and highlighted superior
690 robustness of the spectrophotometric over the electrochemical detection.
691 • Quantifying changes in the EDC of DOM during chemical oxidation,
692 particularly when combined with monitoring changes in UV absorbance,
693 provides a direct means to monitor loss of electron-donating aromatic moieties
694 in DOM during chemical oxidation and provides insights into the distinct
695 chemical pathways by which DOM is oxidized by different chemical oxidants.
696 In water treatment facilities, monitoring of EDC will help to adjust oxidant
697 doses to variations in the contents of activated aromatic moieties in the DOM
698 and hence the oxidant demand.

Acknowledgements

LÖ acknowledges the Swedish Research Council VR for financial support (project no 2014-6839). The authors acknowledge Jaqueline Traber at Eawag for performing SEC-OCD measurements. MS and NW thank the Swiss National Science Foundation (Project 591 200020_159692) for funding and ETH Zurich for financing the FIA system (Scientific Equipment Program).

Appendix A. Supplementary Material

Supplementary Material related to this article can be found at […].

References

Aeschbacher, M., Graf, C., Schwarzenbach, R.P. and Sander, M. (2012) Antioxidant Properties of Humic Substances. Environmental Science & Technology 46(9), 4916-4925.

Aeschbacher, M., Sander, M. and Schwarzenbach, R.P. (2010) Novel Electrochemical Approach to Assess the Redox Properties of Humic Substances. Environmental Science & Technology 44(1), 87-93.

Aeschbacher, M., Vergari, D., Schwarzenbach, R.P. and Sander, M. (2011) Electrochemical Analysis of Proton and Electron Transfer Equilibria of the Reducible Moieties in Humic Acids. Environmental Science & Technology 45(19), 8385-8394.

Amy, G. (2008) Fundamental understanding of organic matter fouling of membranes. Desalination 231(1), 44-51.

American Public Health Association (APHA), (2012) Standard Methods for the Examination of Water and Wastewater, 22nd Edition, pp. 4-69 to 4-70, APHA, Washington, DC.

Bader, H. and Hoigné, J. (1981) Determination of ozone in water by the indigo method. Water Research 15(4), 449-456.

Bahr, C., Schumacher, J., Ernst, M., Luck, F., Heinzmann, B. and Jekel, M. (2007) SUVA as control parameter for the effective ozonation of organic pollutants in secondary effluent. Water Science and Technology 55(12), 267-274.

Bourgin, M., Beck, B., Boehler, M., Borowska, E., Fleiner, J., Salhi, E., Teichler, R., von Gunten, U., Siegrist, H. and McArdell, C.S. (2018) Evaluation of a full-scale wastewater treatment plant upgraded with ozonation and biological post-treatments: Abatement of micropollutants, formation of transformation products and oxidation by-products. Water Research 129, 486-498.

Chin, Y.P., Aiken, G. and Oloughlin, E. (1994) Molecular-weight, polydispersity, and spectroscopic properties of aquatic humic substances. Environmental Science & Technology 28(11), 1853-1858.

Chon, K., Lee, Y., Traber, J. and von Gunten, U. (2013) Quantification and characterization of dissolved organic nitrogen in wastewater effluents by

electrodialysis treatment followed by size-exclusion chromatography with nitrogen detection. Water Research 47(14), 5381-5391.
Chon, K., Salhi, E. and von Gunten, U. (2015) Combination of UV absorbance and electron donating capacity to assess degradation of micropollutants and formation of bromate during ozonation of wastewater effluents. Water Research 81, 388-397.
Collins, M.R. and Vaughan, C.W. (1995) Disinfection by-products in water treatment - The chemistry of their formation and control, p. 520, CRC PRESS, Florida, USA.
de Vera, G.A., Gernjak, W. and Radjenovic, J. (2017) Predicting reactivity of model DOM compounds towards chlorine with mediated electrochemical oxidation. Water Research 114, 113-121.
Deborde, M. and von Gunten, U. (2008) Reactions of chlorine with inorganic and organic compounds during water treatment - Kinetics and mechanisms: A critical review. Water Research 42(1-2), 13-51.
Elovitz, M.S., von Gunten, U. and Kaiser, H.-P. (2000) Natural organic matter and disinfection by-products, Characterization and control in drinking water. Barrett, S.E., Krasner, S.W. and Amy, G. (ed), American Chemical Society, Washington, DC.
Escobar, I.C. and Randall, A.A. (2001) Case study: Ozonation and distribution system biostability. Journal American Water Works Association 93(10), 77-89.
Fram, M.S., Fujii, R., Weishaar, J.L., Beramaschi, B.A., Aiken, G.R., (1999) How DOC composition may explain the poor correlation between specific trihalomethane formation potential and specific UV absorbance. U. S. Geol. Surv. Toxic. Subst. Hydrol. Program 2, 99, 4018B (Water Resource Division, US Geological Survey: Sacramento, CA).
Gallard, H. and von Gunten, U. (2002) Chlorination of phenols: Kinetics and formation of chloroform. Environmental Science & Technology 36(5), 884-890.
Hammes, F., Salhi, E., Köster, O., Kaiser, H.-P., Egli, T. and von Gunten, U. (2006) Mechanistic and kinetic evaluation of organic disinfection by-product and assimilable organic carbon (AOC) formation during the ozonation of drinking water. Water Research 40(12), 2275-2286.
Her, N., Amy, G., Foss, D., Cho, J., Yoon, Y. and Kosenka, P. (2002) Optimization of method for detecting and characterizing NOM by HPLC-size exclusion chromatography with UV and on-line DOC detection. Environmental Science and Technology 36(5), 1069-1076.
Hu, J.Y., Wang, Z.S., Ng, W.J. and Ong, S.L. (1999) The effect of water treatment processes on the biological stability of potable water. Water Research 33(11), 2587-2592.
Huber, S.A., Balz, A., Abert, M. and Pronk, W. (2011) Characterisation of aquatic humic and non-humic matter with size-exclusion chromatography - organic carbon detection - organic nitrogen detection (LC-OCD-OND). Water Research 45(2), 879-885.
Kennedy, A.M. and Summers, R.S. (2015) Effect of DOM Size on Organic Micropollutant Adsorption by GAC. Environmental Science & Technology 49(11), 6617-6624.
Köhler, S.J., Lavonen, E., Keucken, A., Schmitt-Kopplin, P., Spanjer, T. and Persson, K. (2016) Upgrading coagulation with hollow-fibre nanofiltration for improved organic matter removal during surface water treatment. Water Research 89, 232-240.
Korshin, G.V., Li, C.W. and Benjamin, M.M. (1997) Monitoring the properties of natural organic matter through UV spectroscopy: A consistent theory. Water Research 31(7), 1787-1795.

786 Krasner, S.W., Mitch, W.A., McCurry, D.L., Hanigan, D. and Westerhoff, P. (2013)
787 Formation, precursors, control, and occurrence of nitrosamines in drinking water: A
788 review. Water Research 47(13), 4433-4450.
789 Lavonen, E.E., Gonsior, M., Tranvik, L.J., Schmitt-Kopplin, P. and Kohler, S.J.
790 (2013) Selective Chlorination of Natural Organic Matter: Identification of Previously
791 Unknown Disinfection Byproducts. Environmental Science & Technology 47(5),
792 2264-2271.
793 Lee, Y. and von Gunten, U. (2016) Advances in predicting organic contaminant
794 abatement during ozonation of municipal wastewater effluent: reaction kinetics,
795 transformation products, and changes of biological effects. Environmental Science-
796 Water Research & Technology 2(3), 421-442.
797 Leenheer, J.A. and Croue, J.P. (2003) Characterizing aquatic dissolved organic
798 matter. Environmental Science & Technology 37(1), 18A-26A.
799 Toshoh Bioscience (2018), Process Media Products, Description of size-exclusion
800 media in SEC columns, Tosoh Bioscience (pdf),
801 https://www.separations.eu.tosohbioscience.com/OpenPDF.aspx?path=/File%20Libra
802 ry/TBG/Products%20Download//Operating%20Conditions%20and%20Specifications
803 /rds4010.pdf, accessed on March 5, 2018.
804 Önnby, L., Salhi, E., McKay, G., Ortiz-Rosario, F. and von Gunten, U. (2018) Ozone
805 and chlorine interactions with dissolved organic matter - assessment of oxidant-
806 reactive moieties by optical measurements and electron donating capacities, in
807 preparation.
808 Pinkernell, U., Luke, H.J. and Karst, U. (1997) Selective photometric determination
809 of peroxycarboxylic acids in the presence of hydrogen peroxide. Analyst 122(6), 567-
810 571.
811 Pinkernell, U., Nowack, B., Gallard, H. and von Gunten, U. (2000) Methods for the
812 photometric determination of reactive bromine and chlorine species with ABTS.
813 Water Research 34(18), 4343-4350.
814 Ramseier, M.K. and von Gunten, U. (2009) Mechanisms of Phenol Ozonation-
815 Kinetics of Formation of Primary and Secondary Reaction Products. Ozone-Science
816 & Engineering 31(3), 201-215.
817 Richardson, S.D. (2003) Disinfection by-products and other emerging contaminants
818 in drinking water. Trac-Trends in Analytical Chemistry 22(10), 666-684.
819 Richardson, S.D. (2011) Encyclopedia of Environmental Health. Nriago, J.O. (ed),
820 pp. 110-136, Elsevier Sciece Inc, Burlington, MA.
821 Richardson, S.D., Plewa, M.J., Wagner, E.D., Schoeny, R. and DeMarini, D.M.
822 (2007) Occurrence, genotoxicity, and carcinogenicity of regulated and emerging
823 disinfection by-products in drinking water: A review and roadmap for research.
824 Mutation Research-Reviews in Mutation Research 636(1-3), 178-242.
825 Scott, S.L., Chen, W.J., Bakac, A. and Espenson, J.H. (1993) Spectroscopic
826 parameters, electrode potentials, acid ionization constants, and electron exchange
827 rates of the 2,2'-azinobis(3-ethylbenzothiazoline-6-sulfonate) radicals and ions. The
828 Journal of Physical Chemistry 97(25), 6710-6714.
829 Soulard, M., Bloc, F. and Hatterer, A. (1981) Diagrams of Existence of Chloramines
830 and Bromamines in Aqueous-Solution. Journal of the Chemical Society-Dalton
831 Transactions (12), 2300-2310.
832 Stenson, A.C., Marshall, A.G. and Cooper, W.T. (2003) Exact masses and chemical
833 formulas of individual Suwannee River fulvic acids from ultrahigh resolution
834 electrospray ionization Fourier transform ion cyclotron resonance mass spectra.
835 Analytical Chemistry 75(6), 1275-1284.

836 Traina, S.J., Novak, J. and Smeck, N.E. (1990) An ultraviolet absorbance methods of
837 estimating the percent aromatic carbon content of humic acids. Journal of
838 Environmental Quality 19(1), 151-153.
839 Van der Kooij, D., Hijnen, W.A.M. and Kruithof, J.C. (1989) The effects of
840 ozonation, biological filtration and distribution on the concentration of easily
841 assimilable organic-carbon (AOC) in drinking-water. Ozone-Science & Engineering
842 11(3), 297-311.
843 Velten, S., Knappe, D.R.U., Traber, J., Kaiser, H.-P., von Gunten, U., Boller, M. and
844 Meylan, S. (2011) Characterization of natural organic matter adsorption in granular
845 activated carbon adsorbers. Water Research 45(13), 3951-3959.
846 von Gunten, U. (2003) Ozonation of drinking water: Part II. Disinfection and by-
847 product formation in presence of bromide, iodide or chlorine. Water Research 37(7),
848 1469-1487.
849 von Sonntag, C. and von Gunten, U. (2012) Chemistry of ozone in water and
850 wastewater treatment: From basic principles to applications, IWA Publishing,
851 London, UK.
852 Walpen, N., Getzinger, G.J., Schroth, M.H. and Sander, M. (2018) Electron-donating
853 Phenolic and Electron-accepting Quinone Moieties in Peat Dissolved Organic Matter:
854 Quantities, Redox Transformations, and Implications for Peat Biogeochemistry.
855 Submitted to Environ. Sci. Technol.
856 Walpen, N., Schroth, M.H. and Sander, M. (2016) Quantification of Phenolic
857 Antioxidant Moieties in Dissolved Organic Matter by Flow-Injection Analysis with
858 Electrochemical Detection. Environmental Science & Technology 50(12), 6423-6432.
859 Weishaar, J.L., Aiken, G.R., Bergamaschi, B.A., Fram, M.S., Fujii, R. and Mopper,
860 K. (2003) Evaluation of Specific Ultraviolet Absorbance as an Indicator of the
861 Chemical Composition and Reactivity of Dissolved Organic Carbon. Environmental
862 Science & Technology 37(20), 4702-4708.
863 Wenk, J., Aeschbacher, M., Salhi, E., Canonica, S., von Gunten, U. and Sander, M.
864 (2013) Chemical Oxidation of Dissolved Organic Matter by Chlorine Dioxide,
865 Chlorine, And Ozone: Effects on Its Optical and Antioxidant Properties.
866 Environmental Science & Technology 47(19), 11147-11156.
867 Wert, E.C., Rosario-Ortiz, F.L. and Snyder, S.A. (2009) Using Ultraviolet
868 Absorbance and Color To Assess Pharmaceutical Oxidation during Ozonation of
869 Wastewater. Environmental Science & Technology 43(13), 4858-4863.
870 Westerhoff, P., Aiken, G., Amy, G. and Debroux, J. (1999) Relationships between the
871 structure of natural organic matter and its reactivity towards molecular ozone and
872 hydroxyl radicals. Water Research 33(10), 2265-2276.
873 Yuan, W. and Zydney, A.L. (1999) Humic acid fouling during microfiltration. Journal
874 of Membrane Science 157(1), 1-12.
875 Zhang, X.R. and Minear, R.A. (2006) Formation, adsorption and separation of high
876 molecular weight disinfection byproducts resulting from chlorination of aquatic
877 humic substances. Water Research 40(2), 221-230.

878

879

880

881

Figure 1. Schematic designs of the two analytical system setups used to quantify the changes in the electron donating capacity (EDC) of model DOM isolates and real water samples during ozonation or chlorination: the SEC-EDC (top) is based on size exclusion chromatography (SEC) and the FIA-EDC (bottom) is based on flow-injection analysis.

Figure 2. Absorbance measured at 254 nm for the three DOM isolates (SRFA, PLFA, and NNOM) eluting from the size exclusion chromatography (SEC) column on the SEC-EDC system. The concentrations of the analyzed DOM solutions were 2 $mg_C \cdot L^{-1}$ for all three DOM samples. The absorbance of each DOM is normalized to the total area of its elution peak.

Figure 3. Linearity in the absorbance and oxidative current response on the SEC-EDC and FIA-EDC systems, respectively, for injections of the model DOM isolate SRFA. (a) Increases in the heights of the absorbance loss peaks at 405 nm on the SEC-EDC system with increasing injected amounts of SRFA (injected carbon masses from m_C= 1.25 to 7.5 μg_C). The absorbance loss peaks resulted from the reduction of $ABTS^{\bullet+}$ by electron-donating (i.e., oxidizable) moieties in SRFA. (b) Linear increase in the areas under the negative absorbance peaks on the SEC-EDC system (shown in panel a) with increasing injected amounts of SRFA. (c) Oxidative current responses on the FIA-EDC system for injections of increasing amounts of SRFA (injected carbon masses from m_C= 0.19 to 0.93 μg_C) and of decreasing injected amounts of the redox standard ascorbate (electron donating capacity of EDC= 2.00 $mol_{e^-} \cdot mol_{ascorbate}^{-1}$) used to calibrate the FIA-EDC system response for absolute EDC quantification of DOM samples. (d) Linear increases in the areas of the oxidative current peaks (shown in panel c) with increasing amounts of SRFA injected into the FIA-EDC system. The linear regression curve corresponds to an EDC of SRFA of 5.75 ± 0.19 $mmol_{e^-}\ g_C^{-1}$.

Figure 4. Changes in the electron donating capacities (EDC) of the DOM isolates SRFA (blue squares), PLFA (red circles), and NNOM (green triangles) upon chemical oxidation at different specific doses of (a, b) ozone and (c, d) chlorine (HOCl), analyzed on (a,c) the SEC-EDC system and (b, d) the FIA-EDC system. All EDC of DOM isolates reacted with a specific oxidant dose are reported relative to the EDC of the respective untreated DOM, EDC_0. The DOM samples were chemically oxidized in pH 7 buffer (10 mM phosphate) and in the presence of *t*-BuOH (100 mM; for both ozonation and chlorination). The concentration of all three model DOM isolates was 2.5 $mg_C \cdot L^{-1}$ (corresponding to 0.208 $mmol_C \cdot L^{-1}$). The EDC of PLFA and NNOM samples treated with the highest specific HOCl dose are not shown because their responses were too small to be accurately analyzed.

Figure 5. Changes in the relative electron donating capacities (EDC) of the DOM from natural and engineered aquatic systems, SLW (purple diamonds), VLW (orange triangles), and WWE (brown inverted triangles) upon chemical oxidation at different specific doses for (a, b) ozone and (c, d) chlorine (HOCl), analyzed on (a, c) the SEC-EDC system and (b, d) the FIA-EDC system. All EDC of DOM samples reacted with a specific oxidant dose are reported relative to the EDC of the respective untreated DOM samples, EDC_0. The DOM samples were chemically oxidized in pH 7 buffer (10 mM phosphate) and in the presence of *t*-BuOH (100 mM; for both ozonation and chlorination). The DOC concentration of all three real water samples was 2.5 $mg_C \cdot L^{-1}$ (i.e., 0.208 $mmol_C \cdot L^{-1}$).

Figure 6. Comparison of the relative decreases in the electron donating capacities (EDC) of DOM samples measured by the FIA-EDC system (y-axis) and the SEC-EDC system (x-axis). All EDC of DOM samples reacted with a specific oxidant dose are reported relative to the EDC of the respective untreated DOM samples, EDC_0. The decreases in EDC are shown for (a, b) model DOM isolates and (c, d) real water DOM during both (a, c) ozonation and (b, d) chlorination. The data is replotted from Figures 4 and 5 above. The grey dashed line represents the 1:1 line (i.e., same relative decreases in EDC for FIA-EDC and SEC-EDC).

Figure 7. Changes in the relative electron donating capacities (EDC) of the DOM isolates SRFA (blue triangles), PLFA (red circles) and NNOM (green squares) quantified on the FIA-EDC system plotted versus the relative changes in the absorbance values at 254 nm (A_{254}) of the same isolates during ozonation and chlorination with different specific oxidant doses (oxidant dose increases as indicated by the arrows in the figure). All EDC and A_{254} values of DOM samples treated with a specific oxidant dose are reported relative to the EDC and A_{254} values of the respective untreated DOM samples, EDC_0 and $A_{254,\,0}$, respectively.

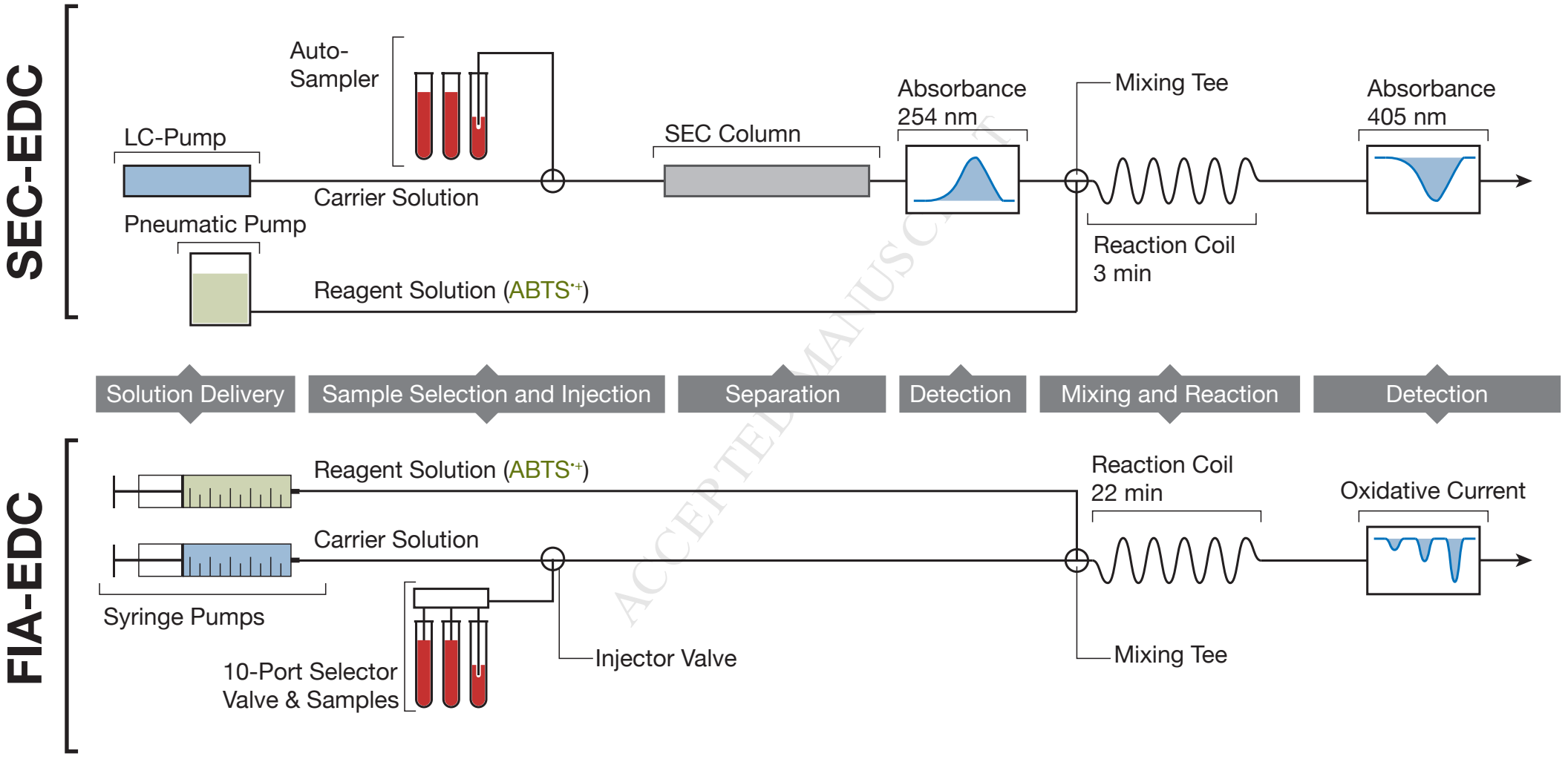

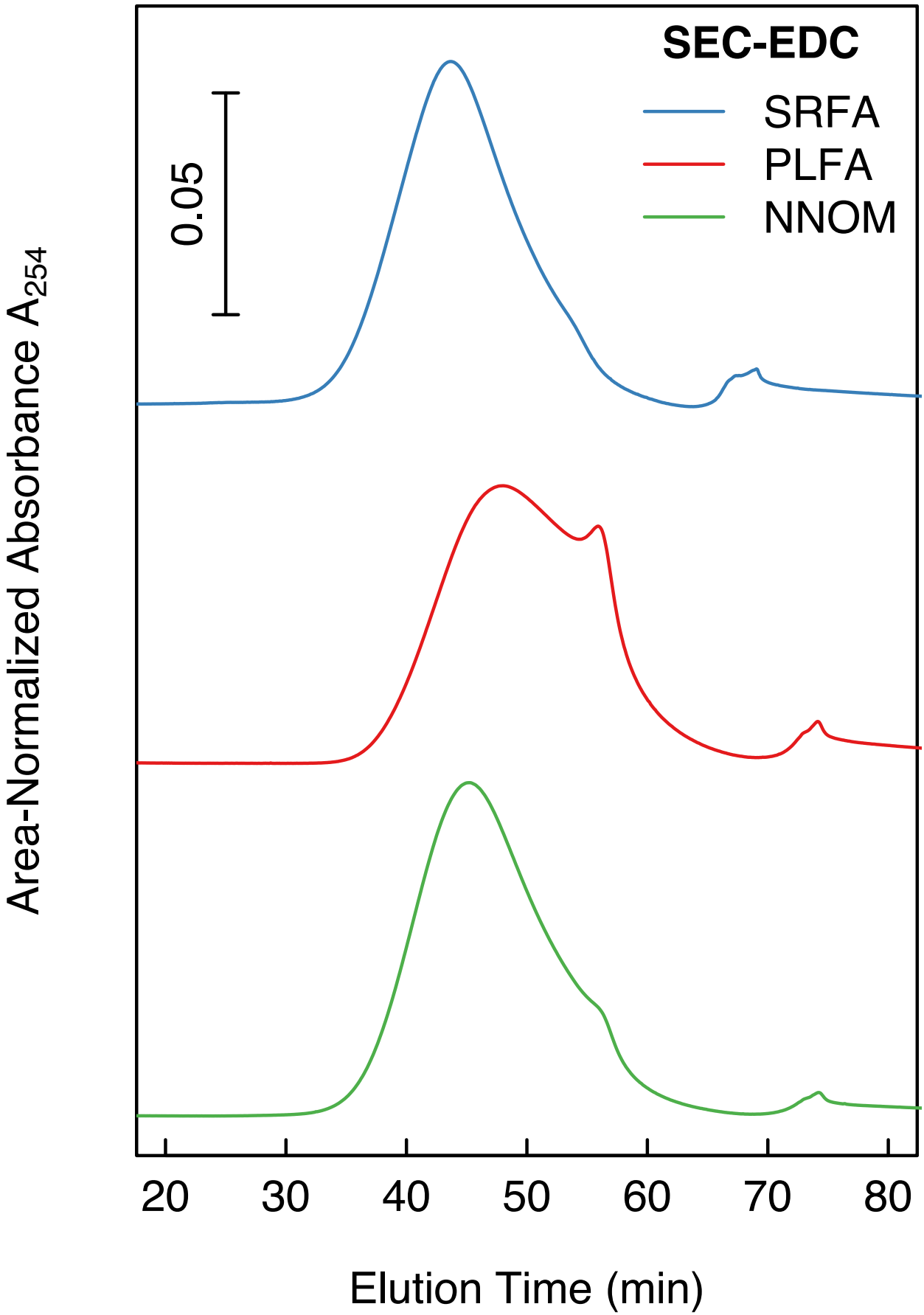
SEC-EDC
SRFA
PLFA
NNOM
0.05
Area-Normalized Absorbance A_{254}
20
30
40
50
60
70
80
Elution Time (min)

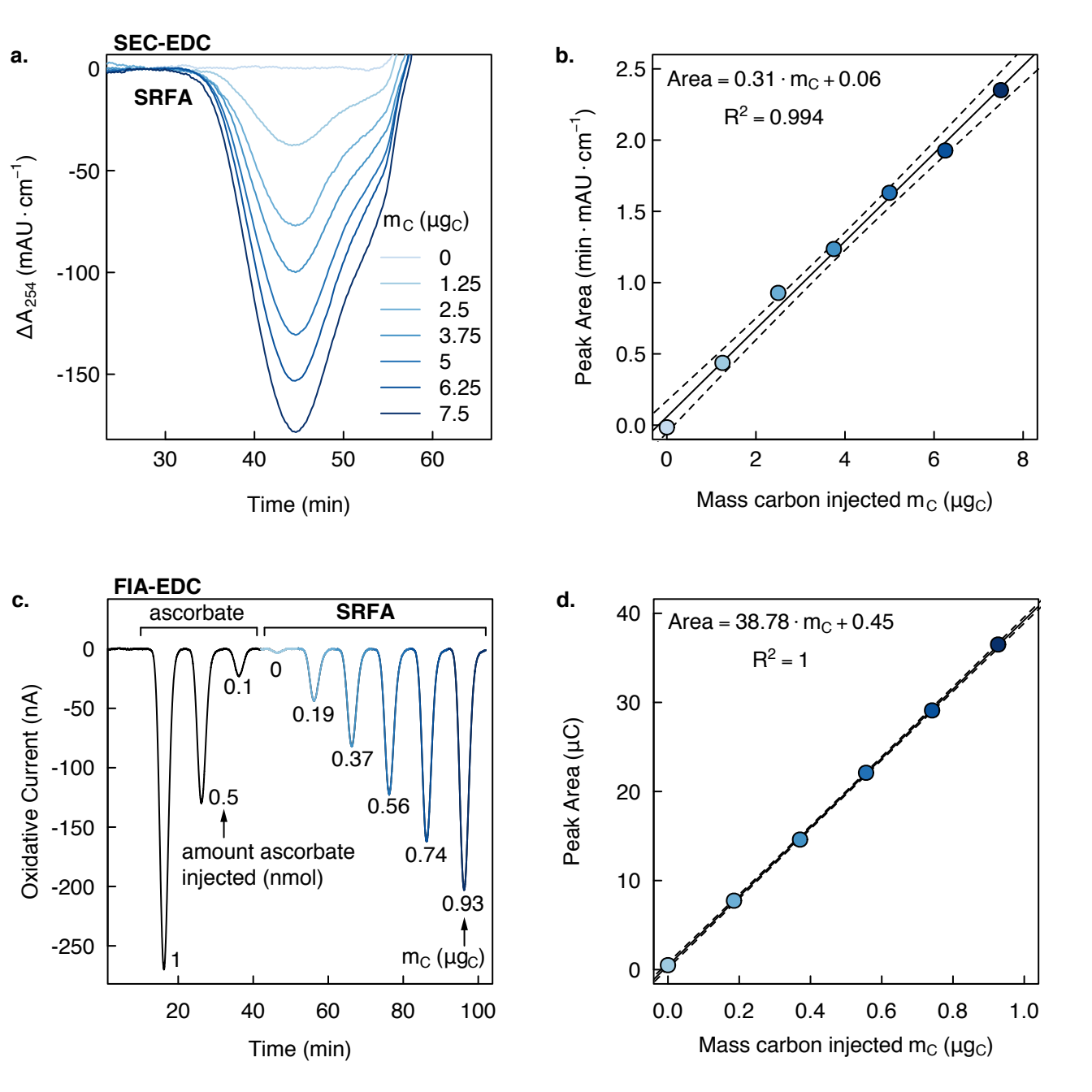
a.
SEC-EDC
SRFA
ΔA_{254} (mAU · cm^{-1})
Time (min)
m_C (µg$_C$)
0
1.25
2.5
3.75
5
6.25
7.5
b.
Area = 0.31 · m_C + 0.06
R^2 = 0.994
Peak Area (min · mAU · cm^{-1})
Mass carbon injected m_C (µg$_C$)
c.
FIA-EDC
ascorbate
SRFA
Oxidative Current (nA)
amount ascorbate injected (nmol)
m_C (µg$_C$)
Time (min)
d.
Area = 38.78 · m_C + 0.45
R^2 = 1
Peak Area (µC)
Mass carbon injected m_C (µg$_C$)

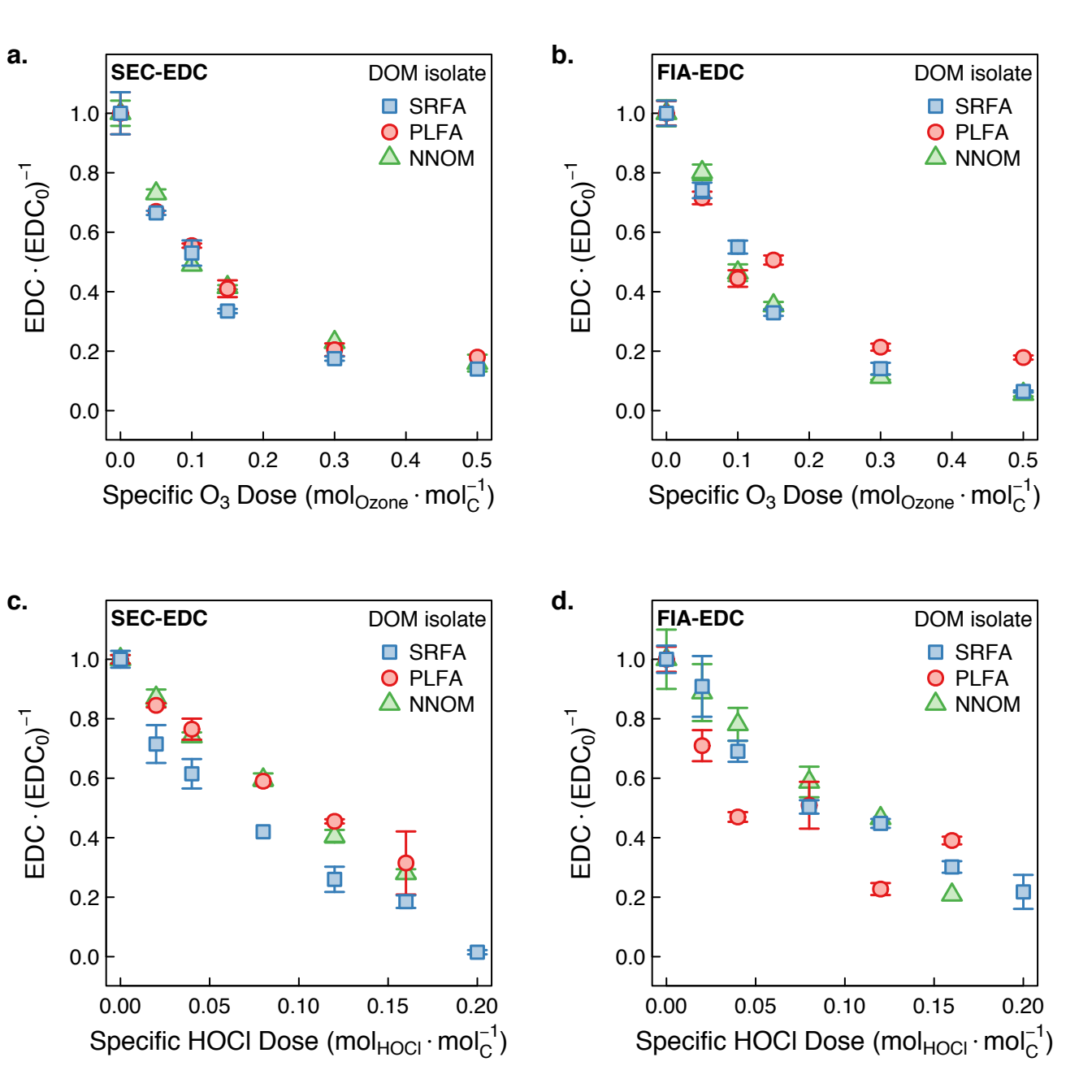
a.
SEC-EDC
DOM isolate
SRFA
PLFA
NNOM
EDC · (EDC0)−1
1.0
0.8
0.6
0.4
0.2
0.0
0.0
0.1
0.2
0.3
0.4
0.5
Specific O3 Dose (molOzone · molC−1)
b.
FIA-EDC
DOM isolate
SRFA
PLFA
NNOM
EDC · (EDC0)−1
1.0
0.8
0.6
0.4
0.2
0.0
0.0
0.1
0.2
0.3
0.4
0.5
Specific O3 Dose (molOzone · molC−1)
c.
SEC-EDC
DOM isolate
SRFA
PLFA
NNOM
EDC · (EDC0)−1
1.0
0.8
0.6
0.4
0.2
0.0
0.00
0.05
0.10
0.15
0.20
Specific HOCl Dose (molHOCl · molC−1)
d.
FIA-EDC
DOM isolate
SRFA
PLFA
NNOM
EDC · (EDC0)−1
1.0
0.8
0.6
0.4
0.2
0.0
0.00
0.05
0.10
0.15
0.20
Specific HOCl Dose (molHOCl · molC−1)

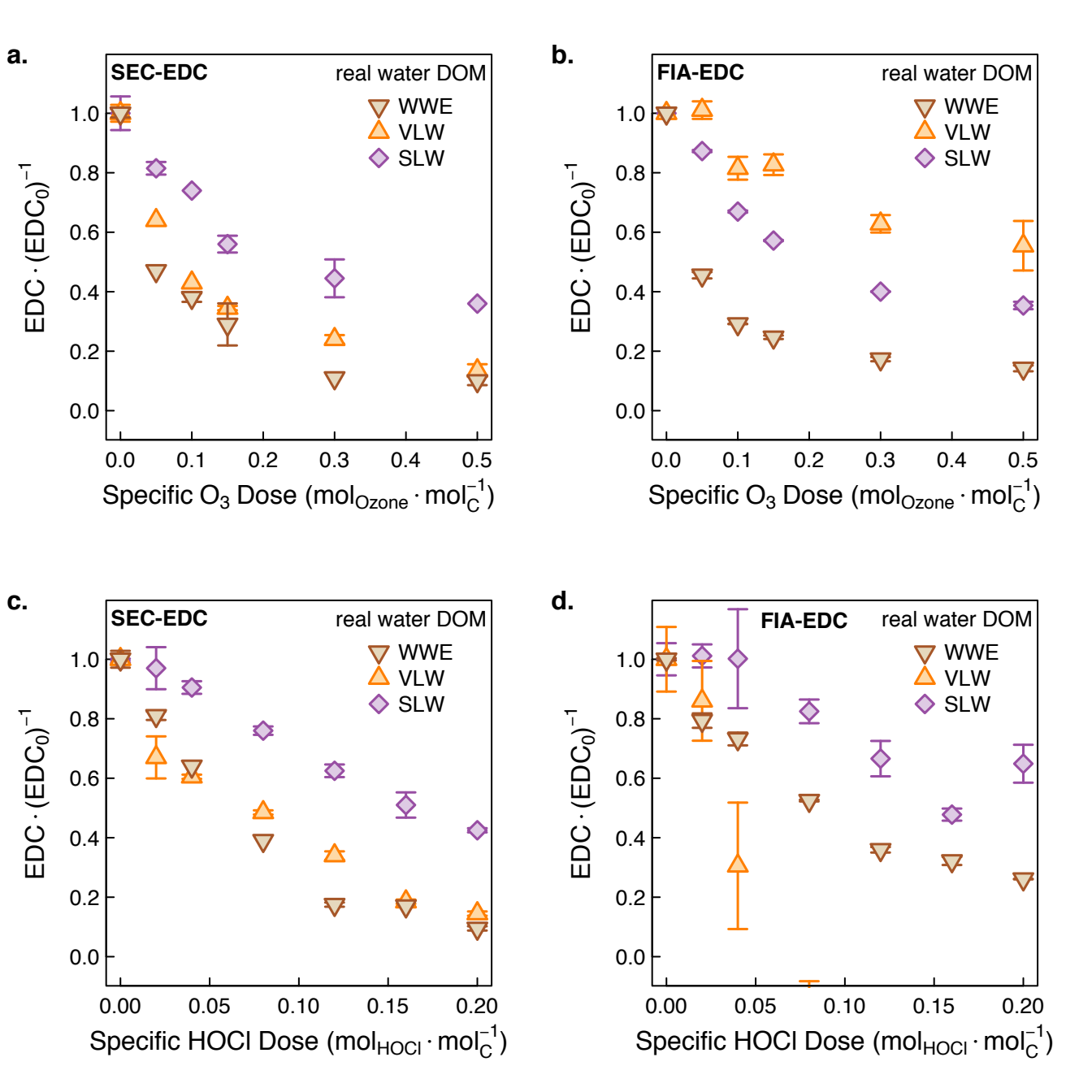
a.
SEC-EDC
real water DOM
WWE
VLW
SLW
EDC · (EDC0)−1
Specific O3 Dose (molOzone · molC−1)
b.
FIA-EDC
real water DOM
WWE
VLW
SLW
EDC · (EDC0)−1
Specific O3 Dose (molOzone · molC−1)
c.
SEC-EDC
real water DOM
WWE
VLW
SLW
EDC · (EDC0)−1
Specific HOCl Dose (molHOCl · molC−1)
d.
FIA-EDC
real water DOM
WWE
VLW
SLW
EDC · (EDC0)−1
Specific HOCl Dose (molHOCl · molC−1)

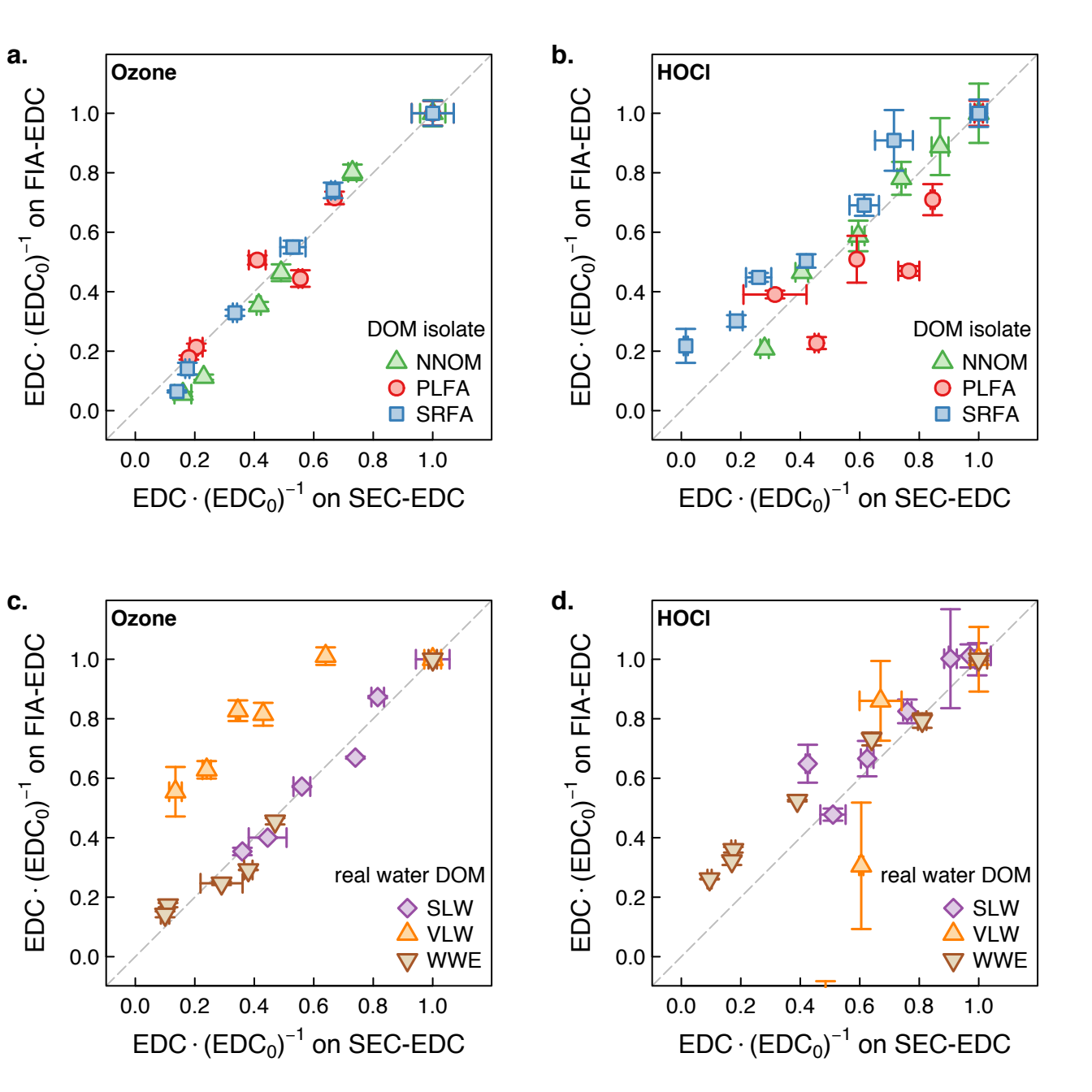
a.
Ozone
DOM isolate
NNOM
PLFA
SRFA
b.
HOCl
DOM isolate
NNOM
PLFA
SRFA
c.
Ozone
real water DOM
SLW
VLW
WWE
d.
HOCl
real water DOM
SLW
VLW
WWE
EDC · (EDC0)−1 on FIA-EDC
EDC · (EDC0)−1 on SEC-EDC
0.0
0.2
0.4
0.6
0.8
1.0

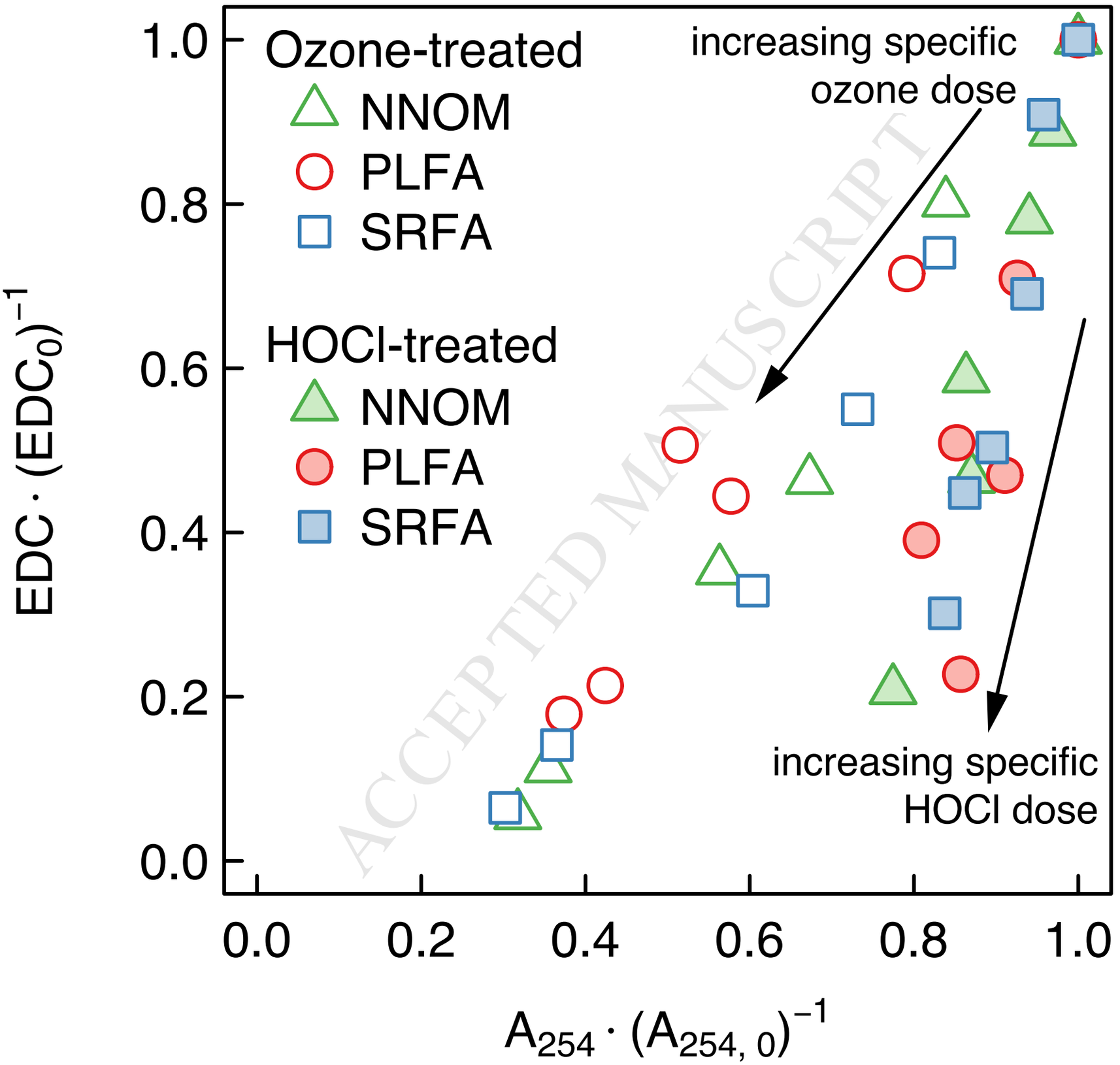

Highlights

- Determination of electron-donating capacity (EDC) in DOM by two analytical methods
- EDC is a quantitative measure of activated aromatic moieties in DOM, including phenols
- High sensitivity of methods allows analysis of dilute DOM samples (<1 $mg_C \cdot L^{-1}$)
- Ozonation and chlorination results in dose- and oxidant-dependent EDC decreases
- EDC provides a means to assess oxidant reactivity with DOM and adjust oxidant dosing

Monitoring Chemical Oxidation of Dissolved Organic Matter (DOM)